CrossMark

ORIGINAL ARTICLE

Estimating aboveground carbon using airborne LiDAR in Cambodian tropical seasonal forests for REDD+ implementation

Tetsuji Ota[1] · Tsuyoshi Kajisa[2] · Nobuya Mizoue[1] · Shigejiro Yoshida[1] ·
Gen Takao[3] · Yasumasa Hirata[3] · Naoyuki Furuya[4] · Takio Sano[5] ·
Raul Ponce-Hernandez[6] · Oumer S. Ahmed[6] · Heng Sokh[7] · Vuthy Ma[7] ·
Eriko Ito[4] · Jumpei Toriyama[3] · Yukako Monda[3] · Hideki Saito[3] · Yoshiyuki Kiyono[3] ·
Sophal Chann[7] · Nang Ket[7]

Abstract We developed an empirical model to estimate aboveground carbon density with variables derived from airborne Light Detection and Ranging (LiDAR) in tropical seasonal forests in Cambodia, and assessed the effects of LiDAR pulse density on the accurate estimation of aboveground carbon density. First, we tested the applicability of variables used for estimating aboveground carbon density with the original LiDAR pulse density data (26 pulse m^{-2}). Aboveground carbon density was regressed against variables derived from airborne LiDAR. Three individual height variable models were developed along with a canopy density model, and three other models combined canopy height and canopy density variables. The influence of forest type on model accuracy was also assessed. Next, the relationship between pulse density and estimation accuracy was investigated using the best regression model. The accuracy of the models were compared based on seven LiDAR point densities consisting of 0.25, 1, 2, 3, 4, 5 and 10 pulse m^{-2}. The best model was obtained using the single mean canopy height (MCH) model ($R^2 = 0.92$) with the original pulse density data. The relationship between MCH and aboveground carbon density was found to be consistent under different forest types. The differences between predicted and measured residual mean of squares of deviations were less than 1.5 Mg C ha^{-1} between each pulse density. We concluded that aboveground carbon density can be estimated using MCH derived from airborne LiDAR in tropical seasonal forests in Cambodia even with a low pulse density of 0.25 pulse m^{-2} without stratifying the study area based on forest type.

Keywords Aboveground carbon density · Airborne LiDAR · Pulse density · Tropical seasonal forest

✉ Tetsuji Ota
chochoji1983@gmail.com

1 Faculty of Agriculture, Kyushu University, 6-10-1 Hakozaki, Fukuoka 812-8581, Japan

2 Faculty of Agriculture, Kagoshima University, Korimoto 1-21-24, Kagoshima 890-8580, Japan

3 Forestry and Forest Products Research Institute, 1 Matsunosato, Tsukuba 305-8687, Japan

4 Hokkaido Research Center, Forestry and Forest Products Research Institute, 7 Hitsujigaoka, Toyohiraku, Sapporo 062-8516, Japan

5 Asia Air Survey Co., Ltd., Shinyuri 21 Building, 1-2-2 Manpukuji, Asao-ku, Kawasaki 215-0004, Japan

6 Department of Geography, Geomatics, Remote Sensing and Land Resources Laboratory, Trent University, Peterborough, ON K9J 7B8, Canada

7 Forestry Administration, Khan Sen Sok, Phnom Penh, Cambodia

Introduction

Tropical forests play an important role in carbon sequestration in the biosphere (Saatchi et al. 2011; Baccini et al. 2012). However, the expansion of agriculture, destructive logging activities, and other anthropogenic activities continuously cause deforestation and degradation of tropical forests (Geist and Lambin 2001, 2002). In particular, Cambodia's tropical seasonal forests, which are mainly dominated by lowland evergreen forest, semi-evergreen forest and deciduous forest, have been dramatically deforested and degraded. For example, in 1965, 73.04 % of the total land area of Cambodia had forest cover; however, this declined to 59.09 % by 2006 (FAO 2010). Carbon

emissions caused by tropical deforestation and forest degradation comprise an important part of the global carbon budget (Canadell et al. 2007; Le Quéré et al. 2009; Houghton 2012). One mitigation mechanism known as Reducing Emissions from Deforestation and forest Degradation+ (REDD+) aims not only to reduce emissions from deforestation and forest degradation, but also to contribute to the conservation and enhancement of forest carbon stocks, as well as to stimulate sustainable forest management.

REDD+ activities need to be scientifically based while using a robust forest monitoring system (Böttcher et al. 2009). Remote sensing is expected to play an important role in future monitoring for REDD+. Airborne Light Detection and Ranging (LiDAR) is an active remote sensing system suited to collect forest information (Drake et al. 2002, 2003; Anderson et al. 2006; Chen et al. 2007; Donoghue et al. 2007; Falkowski et al. 2009; Zhao and Popescu 2009; Morsdorf et al. 2010). In the tropics, Asner et al. (2010) demonstrated the effectiveness of REDD+ monitoring methods using airborne LiDAR in combination with field data and other remote sensing data. They assessed the capability of variables derived from airborne LiDAR to estimate the aboveground carbon for tropical rain forests in Columbia, Madagascar, Panama and Peru (Asner et al. 2009, 2012a, b; Mascaro et al. 2011). However, tropical rain forests in areas mainly composed of evergreen trees provided the main research sites in the above studies. Few studies have focused on the tropical seasonal forests in Southeast Asia that are composed of forests dominated by mixed evergreen and deciduous trees. In general, an empirical equation is used for estimating aboveground carbon density. Therefore, the calibration of parameters of the equation between aboveground carbon density and the variables derived from airborne LiDAR is necessary. Parameters of the equation sometimes differ depending on forest type (Kronseder et al. 2012). This process may be difficult in the case of tropical seasonal forests, where several forest types are intricately distributed and mixed, because the calibration process needs to be done for each forest type. Consequently, few studies have evaluated the importance of forest type for estimating forest carbon density in seasonal tropical forests.

Data acquisition costs create a major area of concern during the implementation of REDD+ monitoring. LiDAR pulse density is directly related to acquisition cost, being inextricably linked to the time the aircraft/sensor spends flying. A few studies have examined the relationship between the accurate estimation of forest measurement variables (e.g., stand volume and tree height at the stand level) and pulse density (e.g., Magnusson et al. 2007; Gobakken and Næsset 2008; Tesfamichael et al. 2010; Jakubowski et al. 2013). However, these studies mainly focused on boreal or temperate forests and this type of research has not yet been conducted in unmanaged forest in a tropical region.

The objective of this research was to conduct a detailed investigation into the nature of the accuracy of carbon density estimates that can be produced with airborne LiDAR, when applied to both evergreen and deciduous forests in Cambodia. The specific goals of this study were to: (1) develop an empirical model that can be used to estimate aboveground carbon density with variables derived from airborne LiDAR, and to assess whether the accuracy of estimates produced with the empirical model are comparable to those obtained from previous research in these types of rainforests, (2) evaluate the importance of forest type for estimating forest carbon density in seasonal tropical forests, and (3) assess the effect of pulse density of airborne LiDAR on the accurate estimation of aboveground carbon density.

Materials and methods

Study area

The study area, located in Kampong Thom Province in central Cambodia, lies within a province having a total land area of 12,447 km^2 , covering about 7 % of Cambodia (Fig. 1; DFW 1999); it features relatively uniform
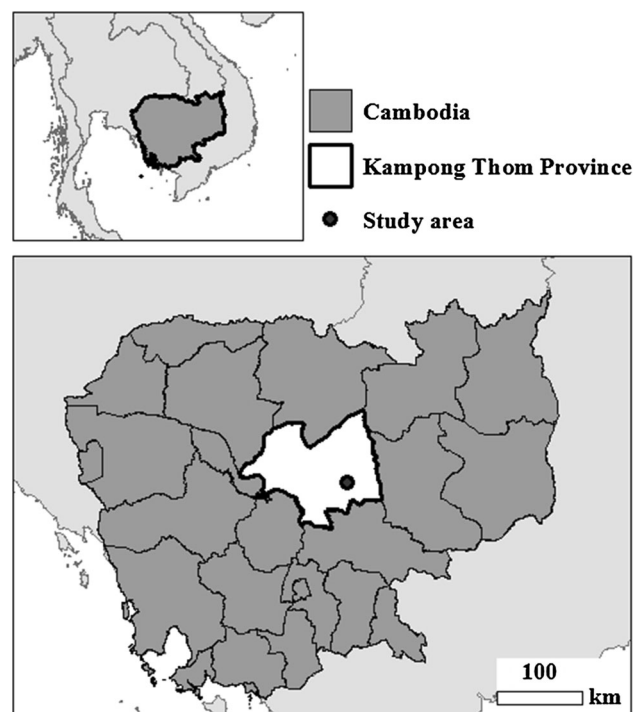

Fig. 1 Vicinity map of the study area in Kampong Thom Province, Cambodia

ecological and geographical conditions. The humidity ranges between 72 and 87 % throughout the year, with an annual mean of 80 % (MRD/GTZ 1985).

Four forest types cover the study area; namely, evergreen, deciduous, and degraded evergreen forest as well as an area of forest re-growth. While dense evergreen forest has a dominant tree height of 30–40 m, the same height is only 10–15 m in sparsely forested deciduous forest. An area of forest re-growth typically forms after clearcutting, with few residual trees left standing. Selective logging causes the degraded evergreen forest in this region to support fewer large trees than evergreen forest, but the landscape still retains its forested nature.

Field sample plots

The permanent plots in each forest type of this study were established as a part of a different series of ongoing field studies. The number of plots in evergreen, deciduous, regrowth and degraded forest were ten, eight, eight and four, respectively. Within each plot, field data were collected under leaf-on canopy conditions between November 2011 and March 2012, including diameter at breast height (DBH), height, and tree position (Table 1), and all trees with DBH > 5 cm were measured. The plot corner coordinates (x, y) were determined using a Global Positioning System (GPS; GPSmap 62 s, Garmin, Olathe, KS, USA). Data collected by this GPS instrument were not differentially corrected; therefore, the accuracy of GPS data was open to question. As a result, these coordinates were field verified in May 2013. In addition, the revised data were used to create tree position maps and ortho-rectified aerial photographs acquired simultaneously with airborne LiDAR. This second method of location verification allowed us to select the most reliable GPS corner coordinates for each plot by comparing them with the tree position maps, aerial photographs, and forest structure in the field. From the selected corner with carefully defined accuracy, we determined the other corners mathematically from the size and the azimuth direction data collected from each plot in the field.

Three sizes of permanent plots were used. Eight regrowth plots and four deciduous forest plots employed

2500 m² (50 m × 50 m) plots. Five evergreen and two deciduous forests plots employed 1200 m² (30 m × 40 m) plots. Four degraded forest and two deciduous forest plots employed 900 m² (30 m × 30 m) plots. Aboveground biomass for each measured tree was calculated using general allometric equations (Brown 1997). Aboveground carbon density was obtained from multiplying the aboveground biomass by 0.50. Plot level aboveground carbon was then calculated by summing aboveground carbon of each tree and divided by the plot size.

LiDAR data

In January 2012, LiDAR data were acquired under leaf-on canopy conditions from a helicopter using ALTM 3100 from Optech, Inc. (Kiln, MS, USA; Table 2). The average density of the first pulse of LiDAR data was 26 pulse m^{-2}.

Methods

LiDAR data thinning

Previous studies have recommended different methods for LiDAR data thinning. The simplest and most commonly used method is random sampling (e.g., Tesfamichael et al. 2010). However, a zigzag LiDAR scan pattern does not result in a random distribution of points, but in semi-regular point distribution (Lovell et al. 2005). The present study followed Gobakken and Næsset (2008) and Magnusson et al. (2007) in selecting one random point within each cell in a grid of regular cells; specifically, we selected

Table 2 Light Detection and Ranging (LiDAR) parameters

Parameter	Optech ALTM 3100
Flight altitude	500 m
Flying speed	25 m s^{-1}
Pulse repetition frequency	100 kHz
Scan frequency	53 Hz
Foot print	0.125 m
Wave length	1064 nm

Table 1 Summary of field measurements

Forest type	n	Aboveground carbon density (Mg C ha^{-1})			Tree height (m)			Stem density (stem ha^{-1})		
		Min	Mean	Max	Min	Mean	Max	Min	Mean	Max
Evergreen	10	88	147	199	1.5	13.2	48.4	1217	1441	1717
Deciduous	8	19	49	75	1.9	7.7	22.9	344	820	1333
Degraded	4	48	66	88	3.8	10.5	26.0	1956	2031	2156
Regrowth	8	11	21	45	1.5	8.0	24.9	476	982	1744

points of 0.10, 0.20, 0.25, 0.33, 0.50, 1.00 and 4.00 m^2 (0.25, 1, 2, 3, 4, 5 and 10 pulse m^{-2}). Finally, this study compared eight LiDAR point densities consisting of seven thinned point densities and the original pulse density.

Creation of digital elevation models (DEMs)

The last return-to-sensor data from each thinned data set and original density data set were used to model the ground surface by filtering earlier returns. In the filtering process, the local minima, assumed to represent the ground, were collected. A suite of DEMs were then generated using natural neighbour interpolation with a spatial resolution of 5 m. Consequently, eight different DEMs were created for eight LiDAR pulse densities.

LiDAR-derived variable calculation

All thinned first and original pulse points were spatially registered to DEMs based on their coordinates. The relative height of each point was computed as the difference between the height of the first return and DEMs. For thinned first pulse points, two different DEMs for each thinning level were used, i.e., the DEMs created from the original and from the corresponding pulse density data. Therefore, the effects of different DEMs on the accurate estimation of aboveground carbon density could be examined.

The first pulse points were classified as either canopy or non-canopy return pulses based on their relative height, while using 1 m as the threshold. The first pulse points were classified as canopy returns if the relative height was ≥ the thresholds. Four variables, namely, mean canopy height (the average value of the relative height of canopy returns in each plot, MCH), median canopy height (H_{50}), maximum height (H_{max}) and canopy density (CD), were derived based on the relative height of the first pulse. The canopy density was calculated as the ratio between the number of pulses returned from the canopy and the total number of pulses (Magnusson et al. 2007).

Statistical analysis

A multiple regression model [Eq. (1)] was developed to relate the LiDAR-derived variables to the measured aboveground carbon, based on Næsset (1997, 2002) and Magnusson et al. (2007):

$$C = \beta_0 h^{\beta_1} d^{\beta_2}, \tag{1}$$

where C is the aboveground carbon density in Mg C ha^{-1}, and where β_0, β_1 and β_2 are the regression coefficients, h is the height variable and d is the canopy density obtained from both LiDAR data sets. Additionally, we assessed the influence of forest type on the regression by expanding

Eq. (1) with variables representing forest type as a dummy variable. The expanded Eq. (2) follows:

$$C = \beta_0 h^{\beta_1} d^{\beta_2} \prod_{i=1}^{n-1} e^{b_i z_i}, \tag{2}$$

where b_i is the regression coefficient of ith class, z_i is the dummy variable of ith class and n is the class number. Forest type was expressed using four different groups (i.e., evergreen, deciduous, regrowth and degraded forest); in addition, z_1, z_2 and z_3 were coded 1 for deciduous forest, regrowth, and degraded evergreen forest, respectively, and 0 was coded for other types of forest in each respective group (z_1, z_2 and z_3). We used log transformation to simplify Eq. (2) as a linear regression (Eq. (3)):

$$\log C = \log \beta_0 + \beta_1 \log h + \beta_2 \log d + \sum_{i=1}^{3} b_i z_i \tag{3}$$

Throughout the analysis, the accuracy of estimates of aboveground carbon density was expressed by the coefficient of determination (R^2) using the observed and estimated values of C and the root mean square error (RMSE) expressed in Mg C ha^{-1}. Because of the limited number of field plots, R^2 and RMSE were calculated using leave one-out cross-validation.

First, we checked the applicability of variables to estimate carbon density with the original pulse density data. Aboveground carbon density was regressed against height variables and/or canopy density. Additionally, the pertinence of considering forest type in the analysis was assessed. Then, we selected the best model in terms of R^2, adjusted R^2, RMSE and significance of the regression coefficients. Finally, using the best regression model, the relationship between pulse density and estimation accuracy was investigated using thinned pulse density data. For each thinning level, we tested the DEMs created from both the original and from thinned pulse density data based on Magnusson et al. (2007).

Results

Table 3 summarizes the regression model fit depicting the relationship between carbon density and LiDAR variables with the original pulse density (26 pulse m^{-2}). The accurate estimation, expressed in terms of the RMSE of estimates from the single height, single canopy density and combined models of height variables and canopy density were 17.25–32.40, 56.08, and 16.96–30.52 Mg C ha^{-1}, respectively. The RMSE of the combined model was close to the corresponding single height model. The single MCH model and the combination model of MCH and canopy density were superior to the canopy density model in terms

Table 3 Summary of regression analysis between carbon density and Light Detection and Ranging (LiDAR) variables with original pulse density

Variables	β_0	β_1	β_2	Deciduous	Degraded	Regrowth	R^2	adj R^2	RMSE (Mg C ha^{-1})
MCH	0.90	1.77*					0.92	0.92	17.25
H_{50}	1.23	1.65*					0.91	0.90	18.80
H_{max}	0.02	2.60*					0.74	0.73	32.40
Canopy density	82.51		1.66*				0.23	0.20	56.08
MCH + canopy density	1.10	1.70*	0.20 n.s.				0.92	0.92	16.96
H_{50} + canopy density	1.44	1.60*	0.16 n.s.				0.91	0.90	18.51
H_{max} + canopy density	0.04	2.36*	0.50 n.s.				0.76	0.75	30.52
MCH + forest type	1.57	1.58*		−0.13 n.s.	−0.05 n.s.	−0.26 n.s.	0.92	0.91	17.38
H_{50} + forest type	4.04	1.25*		−0.34*	−0.21 n.s.	−0.57*	0.92	0.91	17.38
H_{max} + forest type	1.62	1.31*		−0.58*	−0.34 n.s.	−1.18*	0.82	0.79	25.88
Canopy density + forest type	153.57		0.69*	−0.88*	−0.86*	−1.86*	0.83	0.80	25.31
MCH + canopy density + forest type	2.26	1.46*	0.31 n.s.	−0.06 n.s.	−0.12 n.s.	−0.30 n.s.	0.92	0.91	16.79
H_{50} + canopy density + forest type	5.42	1.15*	0.26 n.s.	−0.28 n.s.	−0.27 n.s.	−0.61*	0.92	0.91	16.77
H_{max} + canopy density + forest type	2.34	1.21*	0.61*	−0.34 n.s.	−0.39 n.s.	−1.06*	0.84	0.81	24.37

n.s. not significant ($p > 0.05$)

* $p < 0.05$
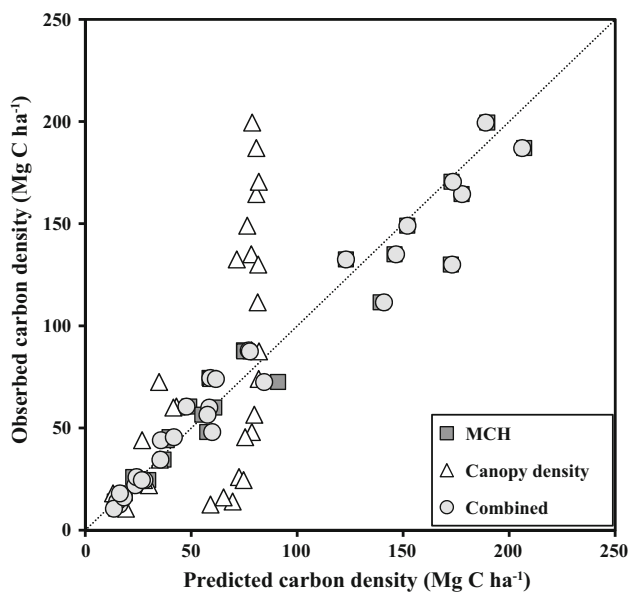
Fig. 2 Predicted values from single MCH, canopy density and combined data. *MCH* mean canopy height

Fig. 3 Relationship between MCH and aboveground carbon density. *MCH* mean canopy height

of RMSE. Both the single MCH model and the combination model of MCH and canopy density explained 92 % of the variation within aboveground carbon density. Canopy density explained less variation of the aboveground carbon density than the MCH model alone. The regression coefficients of canopy density were not significant in the combination model. The predicted values from the single MCH model were very close to the predicted values from the combination of two variables (Fig. 2).
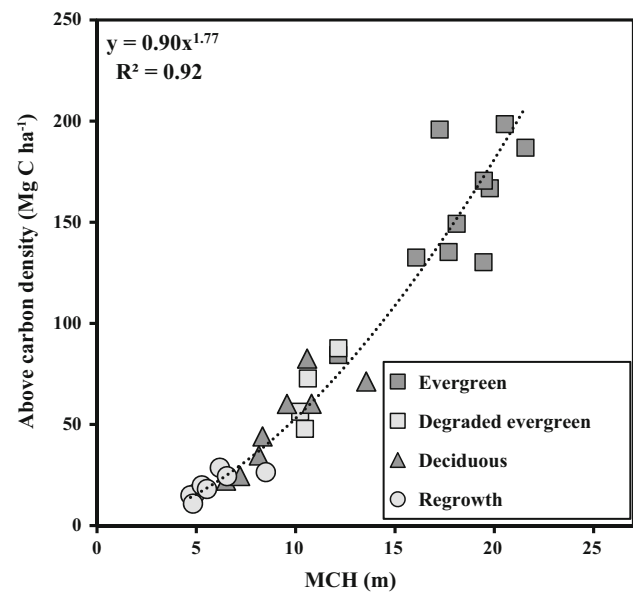
Adding the forest type information improved the accurate estimation of aboveground carbon density in terms of RMSE (Table 3). In particular, the RMSE of the single H_{max} the single canopy density, and H_{max} + canopy density models were dramatically improved by adding the forest type information (Table 3). However, in terms of the adjusted R^2, forest type was not informative except in the case of the single H_{max}, the single canopy density and the H_{max} + canopy density models. In other cases, the
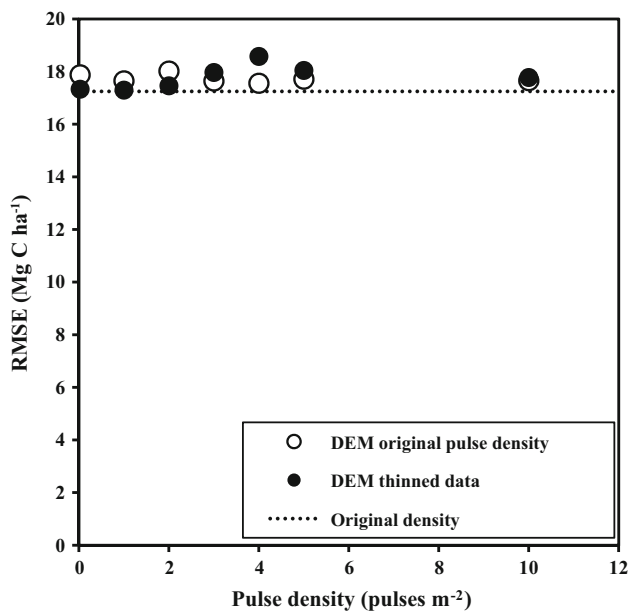
Fig. 4 Relationship between pulse density and RMSE. *DEM* digital elevation model, *RMSE* residual mean of squares of deviations between predicted and measured

adjusted R^2 increased by 0.01 at a maximum even if forest type information was added. The adjusted R^2 of single MCH was the highest after considering forest type.

For all these reasons, we concluded that MCH could explain the aboveground carbon density independent of forest type. In addition, the selected single MCH model with a 1-m threshold was the best model in terms of the resulting RMSE, significance of regression coefficients, and the comparison of the predicted carbon density. Figure 3 shows the relationship between MCH and carbon density in the case of the original pulse density. MCH was found to be highly correlated with aboveground carbon density consistently from low to high MCH, independent of forest type.

Figure 4 shows the relationship between pulse density and the estimation error in terms of the RMSE. A horizontal dotted line indicates the RMSE of the model based on the original pulse density data. RMSE was almost perfectly in line with the pulse density (Fig. 4). The difference between the RMSE of the model from the original pulse density model and from each thinned pulse density model was less than 1.5 Mg C ha^{-1}. Additionally, the variation of

DEMs did not have a considerable impact on RMSE. Both the DEMs created from the original pulse density data and from the thinned pulse density data had almost the same RMSE at each pulse density.

Discussion

In this study, we investigated methods used to accurately estimate aboveground carbon density using different pulse densities of airborne LiDAR in tropical seasonal forests in Cambodia. MCH derived from airborne LiDAR was highly correlated with carbon density (Fig. 2). In the case of tropical forests, several studies have shown how MCH can be used to estimate aboveground carbon in tropical rain forests of Peru, Madagascar and Colombia (Asner et al. 2009, 2010, 2012b, c). The coefficient of determination was between 0.78 and 0.91, and uncertainty was between 17.8 and 23 Mg C ha^{-1} in these studies. Because the coefficient of determination for the best model in our study was 0.92, we can conclude that our estimation of aboveground carbon density in tropical seasonal forest is comparable to that of other biomes.

Canopy density is a useful parameter that can be used to estimate forest variables in tropical rainforest (Ioki et al. 2014). However, our results showed that canopy density explained less variation of the aboveground carbon density than the MCH model alone (Table 3). Also, when the canopy density model was used, the predicted carbon density became saturated (Fig. 2). These results indicate that canopy density has limited usefulness in estimating aboveground carbon density in tropical seasonal forest. One possible reason for this may be that almost every plot in our study area had a closed canopy. Therefore, we conclude that the single MCH model is the best model that can be used to estimate aboveground carbon in tropical seasonal forest.

Accurately estimating aboveground carbon density could be possible using a single allometric equation for the four forest types analysed here (Fig. 3). Similar results were obtained in previous studies of boreal coniferous forest (Næsset 2004) and temperate coniferous forest (Lefsky et al. 2002). Our study demonstrated the ability to estimate aboveground carbon density independently of forest type in tropical seasonal forests. This provides a

Fig. 5 Part of the vertical cross-sectional view of the study area created from airborne LiDAR data
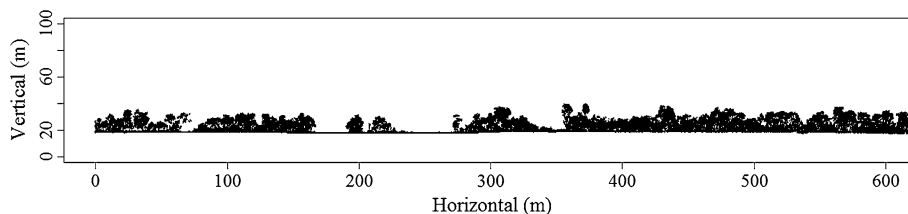
distinct advantage in the case of Cambodia, where several forest types are intricately distributed and mixed, because the calibration of parameters of the equation between aboveground carbon and MCH is not necessary for each individual forest type.

The regression model parameters of the selected model, specifically β_0 and β_1, were 0.90 and 1.77, respectively. Previous studies conducted in tropical forest mainly used this equation: $C = \beta_0 \text{MCH}^{\beta_1}$. The range of β_0 and β_1 in Peru and Madagascar were 0.35–2.97 and 1.31–1.92, respectively (Asner et al. 2010, 2012c). Although our results for β_0 and β_1, 0.90 and 1.77, respectively, are comparable to these previous studies in tropical forests, these values are highly dependent on specific characteristics of the region (e.g., allometric relationship between tree height and DBH). Hence, a calibration process is always required to accurately estimate aboveground carbon density with LiDAR, including laborious and time-consuming forest inventory plots within the LiDAR footprint (Asner 2009). To simplify the calibration process, Asner et al. (2012a) proposed a single airborne LiDAR approach, consisting of a universal model for rainforest, supported by limited input of basal area and wood density data for a given region. This model is based on the empirical relationship between variables derived from LiDAR and forest variables, such as height and basal area from field measurements in Panama, Peru, Madagascar and Hawaii. In this study, we showed that the estimation accuracy and the parameters of the model in Cambodia were comparable to the study in Peru and Madagascar. The universal model for rainforest could be applicable to seasonal tropical forests in Cambodia with the addition of field measurement data to the universal model.

Root mean square error was almost perfectly in line with pulse density. The difference between RMSE of the model from the original pulse density and the models from each thinned pulse density was less than 1.5 Mg C ha^{-1}. Previous studies have shown that pulse density has little or no effect on accuracy for estimating forest variables in boreal forest (Holmgren 2004; Maltamo et al. 2006; Treitz et al. 2012, and temperate forest González-Ferreiro et al. 2012). Because of the limited effect of pulse density in the present study, in agreement with previous studies, we conclude that the effects of pulse density on the accurate estimation of aboveground carbon is also limited in a tropical seasonal forest when the pulse density is changed from 0.25 to 10 pulses m^{-2}, and that low-pulse density LiDAR data are applicable and preferred because of their cost effectiveness and lesser processing time.

Magnusson et al. (2007) assessed the effects on estimation accuracy using different pulse densities derived DEMs and compared the estimation error in terms of RMSE. They showed that the difference in DEM strongly affected the accuracy of forest structure estimation, and that DEMs created from thinned pulse density data had higher RMSE than DEMs created from the original pulse density data. However, in this study, the variation in DEMs had limited effects on aboveground carbon estimation (Fig. 4). In addition, DEMs created from the thinned pulse density data had lower RMSE than DEMs created from the original pulse density data when the pulse density was from 0.25 to 3 pulses m^{-2}. Although the exact reasons are unclear, one possible reason why the difference in DEM had limited effects is that our study area was conducted in a lowland forest on flat land (Fig. 5). More attention needs to be paid to pulse density if the study is conducted in an area of rugged terrain.

The main conclusion of this research is that aboveground carbon density can be accurately estimated from MCH derived from airborne LiDAR in tropical seasonal forests in Cambodia, even using low-pulse density data. Because the relationship between MCH and aboveground carbon density was consistent under the different forest types, aboveground carbon density could be estimated with airborne LiDAR without considering forest type. In the future, the development of a more precise prediction method using a universal model such as that developed by Asner et al. (2012a) is expected.

References

Anderson J, Martin ME, Smith M-L, Dubayah RO, Hofton MA, Hyde P, Peterson BE, Blair JB, Knox RG (2006) The use of waveform lidar to measure northern temperate mixed conifer and deciduous forest structure in New Hampshire. Remote Sens Environ 105:248–261

Asner GP (2009) Tropical forest carbon assessment: integrating satellite and airborne mapping approaches. Environ Res Lett 4:1748–9326

Asner GP, Hughes RF, Varga TA, Knapp DE, Kennedy-Bowdoin T (2009) Environmental and biotic controls over above-ground biomass throughout a tropical rain forest. Ecosystems 12:261–278

Asner GP, Powell GVN, Mascaro J, Knapp DE, Clark JK, Jacobson J, Kennedy-Bowdoin T, Balaji A, Paez-Acosta G, Victoria E, Secada L, Valqui M, Hughes RF (2010) High-resolution forest carbon stocks and emissions in the amazon. Proc Natl Acad Sci USA 107:16738–16742

Asner GP, Mascaro J, Muller-Landau HC, Vieilledent G, Vaudry R, Rasamoelina M, Hall JS, van Breugel M (2012a) A universal airborne LiDAR approach for tropical forest carbon mapping. Oecologia 168:1147–1160

Asner GP, Clark JK, Mascro J, Vaudry R, Chadwick KD, Vieilledent G, Rasamoelina M, Balaji A, Kennedy-Bowdoin T, Maatoug L, Colgan MS, Knapp DE, (2012b) Human and environmental

controls over aboveground carbon storage in Madagascar. Carbon Balance Manag 7. doi:10.1186/1750-0680-7-2

Asner GP, Clark JK, Mascaro J, Galindo García GA, Chadwick KD, Navarrete Encinales DA, Paez-Acosta G, Cabrera Montenegro E, Kennedy-Bowdoin T, Duque Á, Balaji A, Von Hildebrand P, Maatoug L, Phillips Bernal JF, Yepes Quintero AP, Knapp DE, García Dávila MC, Jacobson J, Ordóñez MF (2012c) High-resolution mapping of forest carbon stocks in the Colombian Amazon. Biogeosciences 9:2683–2696

Baccini A, Goetz SJ, Walker WS, Laporte NT, Sun M, Sulla-Menashe D, Hackler J, Beck PSA, Dubayah R, Friedl MA, Samanta S, Houghton RA (2012) Estimated carbon dioxide emissions from tropical deforestation improved by carbon-density maps. Nature Clim Change 2:182–185

Böttcher H, Eisbrenner K, Fritz S, Kindermann G, Kraxner F, McCallum I, Obersteiner M (2009) An assessment of monitoring requirements and costs of reduced emissions from deforestation and degradation. Carbon Balance Manage 4:7. doi:10.1186/1750-0680-4-7

Brown S (1997) Estimating biomass and biomass change in tropical forests: a premier. Food and Agriculture Organization, Forestry Paper, Rome

Canadell JG, Le Quéré C, Raupach MR, Field CB, Buitenhuis ET, Ciais P, Conway TJ, Gillett NP, Houghton RA, Marland G (2007) Contributions to accelerating atmospheric CO2 growth from economic activity, carbon intensity, and efficiency of natural sinks. Proc Natl Acad Sci USA 104:18866–18870

Chen Q, Gong P, Baldocchi DD, Tian Y (2007) Estimating basal area and stem, volume for individual trees from LIDAR data. Photogramm Eng Rem S 73:1355–1365

DFW (1999) Forest cover assessment, Cambodia (in Khmer). Forestry administration of Camodia, Phnom Penh

Donoghue DNM, Watt PJ, Cox NJ, Wilson J (2007) Remote sensing of species mixtures in conifer plantations using Lidar height and intensity data. Remote Sens Environ 110:509–522

Drake JB, Dubayah RO, Clark DB, Knox RG, Blair JB, Hofton MA, Chazdon RL, Weishampel JF, Prince SD (2002) Estimation of tropical forest structural characteristics using large-footprint lidar. Remote Sens Environ 79:305–319

Drake JB, Knox RG, Dubayah RO, Clark DB, ConditR Blair JB, Hofton M (2003) Above-ground biomass estimation in closed canopy Neotropical forests using lidar remote sensing: factors affecting the generality of relationships. Global Ecol Biogeogr 12:147–159

Falkowski MJ, Evans JS, Martinuzzi S, Gessler PE, Hudak AT (2009) Characterizing forest succession with Lidar data: an evaluation for the Inland Northwest, USA. Remote Sens Environ 113:946–956

FAO (2010) Global forest resources assessment 2010: country report Cambodia. Food and Agriculture Organization of the United Nations, Rome

Geist HJ, Lambin EF (2001) What drives tropical deforestation?: a meta-analysis of proximate and underlying causes of deforestation based on subnational case study evidence. LUSS Report Series No. 4

Geist HJ, Lambin EF (2002) Proximate causes and underlying drving gorces of tropical deforestation. Bioscience 52:143–150

Gobakken T, Næsset E (2008) Assessing effects of laser point density, ground sampling intensity, and field sample plot size on biophysical stand properties derived from airborne laser scanner data. Can J For Res 38:1095–1109

González-Ferreiro E, Diéguez-Aranda U, Miranda D (2012) Estimation of stand variables in *Pinus radiata* D. Don plantations using different LiDAR pulse densities. Forestry 85:281–292

Holmgren J (2004) Prediction of tree height, basal area and stem volume in forest stands using airborne laser scanning. Scand J For Res 19:543–553

Houghton RA (2012) Carbon emissions and the drivers of deforestation and forest degradation in the tropics. Curr Opin Environ Sustain 4:597–603

Ioki K, Tsuyuki S, Hirata Y, Phua MH, Wong WVC, Ling ZY, Saito H, Takao G (2014) Estimating above-ground biomass of tropical rainforest of different degradation levels in Northern Borneo using airborne LiDAR. For Ecol Manage 328:335–341

Jakubowski MK, Guo Q, Kelly M (2013) Tradeoffs between lidar pulse density and forest measurement accuracy. Remote Sens Environ 130:245–253

Kronseder K, Ballhorn U, Böhmc V, Siegert F (2012) Above-ground biomass estimation across forest types at different degradation levels in central kalimantan using lidar data. Int J Appl Earth Obs Geoinf 18:37–48

Le Quéré C, Raupach MR, Canadell JG, Marland G, Bopp L, Ciais P, Conway TJ, Doney SC, Feely RA, Foster P, Friedlingstein P, Gurney K, Houghton RA, House JI, Huntingford C, Levy PE, Lomas MR, Majkut J, Metzl N, Ometto JP, Peters GP, Prentice IC, Randerson JT, Running SW, Sarmiento JL, Schuster U, Sitch S, Takahashi T, Viovy N, Van Der Werf GR, Woodward FI (2009) Trends in the sources and sinks of carbon dioxide. Nat Geosci 2:831–836

Lefsky MA, Cohen WB, Harding DJ, Parker GG, Acker SA, Gower ST (2002) Lidar remote sensing of above-ground biomass in three biomes. Global Ecol Biogeogr 11:393–399

Lovell JL, Jupp DLB, Newnham GJ, Coops NC, Culvenor DS (2005) Simulation study for finding optimal lidar acquisition parameters for forest height retrieval. For Ecol Manag 214:398–412

Magnusson M, Fransson JES, Holmgren J (2007) Effects on estimation accuracy of forest variables using different pulse density of laser data. For Sci 53:619–626

Maltamo M, Eerikainen K, Packalen P, Hyyppa J (2006) Estimation of stem volume using laser scanning-based canopy height metrics. Forestry 79:217–229

Mascaro J, Asner GP, Muller-Landau HC, Van Breugel M, Hall J, Dahlin K (2011) Controls over above-ground forest carbon density on barro colorado island, panama. Biogeosciences 8:1615–1629

Morsdorf F, Marell A, Koetz B, Cassagne N, Pimont F, Rigolot E (2010) Discrimination of vegetation strata in a multi-layered Mediterranean forest ecosystem using height and intensity information derived from airborne laser scanning. Remote Sens Environ 114:1403–1415

MRD/GTZ (1985) Regional framework plan Kampong Thom Province. Ministry of Rural Development, Phnom Penh

Næsset E (1997) Estimating timber volume of forest stands using airborne laser scanner data. Remote Sens Environ 61:241–253

Næsset E (2002) Predicting forest stand characteristics with airborne scanning laser using a practical two-stage procedure and field data. Remote Sens Environ 80:88–99

Næsset E (2004) Estimation of above- and below- ground biomass in boreal forest ecosystems. In: Thies M, Kock B, Spiecker H, Weinacker H (eds) Laser-scanners for forest and landscape assessment. International society of photogrammetry and remote sensing. International archeves of photogrammetry, remote sensing and spatial information sciences, Freiburg, pp 145–148

Saatchi SS, Harris NL, Brown S, Lefsky M, Mitchard ETA, Salas W, Zutta BR, Buermann W, Lewis SL, Hagen S, Petrova S, White L, Silman M, Morel A (2011) Benchmark map of forest carbon stocks in tropical regions across three continents. Proc Natl Acad Sci USA 108:9899–9904

Tesfamichael SG, van Aardt JAN, Ahmed F (2010) Estimating plot-level tree height and volume of eucalyptus grandis plantations using small-footprint, discrete return lidar data. Prog Phys Geog 34:515–540

Treitz P, Lim K, Woods M, Pitt D, Nesbitt D, Etheridge D (2012) LiDAR sampling density for forest resource inventories in Ontario, Canada. Remote Sens 4:830–848

Zhao KG, Popescu S (2009) Lidar-based mapping of leaf area index and its use for validating GLOBCARBON satellite LAI product in a temperate forest of the southern USA. Remote Sens Environ 113:1628–1645